Insight into the antimicrobial mechanism of action of þÿ²2,2-amino acid derivatives from molecular dyna simulation : Dancing the can-can at the membrane surface

Koivuniemi, Artturi

2019-11-01

Koivuniemi , A , Fallarero , A & Bunker , A 2019 , ' Insight into the antimicrobial mechanism þÿof action of ²2,2-amino acid derivatives from molecular dynamics simu can-can at the membrane surface ' , Biochimica et Biophysica Acta. Biomembranes , vol. 1861 , no. 11 , 183028 . https://doi.org/10.1016/j.bbamem.2019.07.016

http://hdl.handle.net/10138/307588
https://doi.org/10.1016/j.bbamem.2019.07.016

BBA - Biomembranes 1861 (2019) 183028

Contents lists available at ScienceDirect

BBA - Biomembranes

journal homepage: www.elsevier.com/locate/bbamem

Insight into the antimicrobial mechanism of action of $\beta^{2,2}$-amino acid derivatives from molecular dynamics simulation: Dancing the can-can at the membrane surface

Artturi Koivuniemi, Adyary Fallarero, Alex Bunker*

Centre for Drug Research, Faculty of Pharmacy, University of Helsinki, Helsinki, Finland

ARTICLE INFO

Keywords:
Bacteria
Antibiotic resistance
Antimicrobial peptide
Lipid membrane
Molecular dynamics simulation

ABSTRACT

The development of antimicrobial agents that target and selectively disrupt biofilms is a pressing issue since, so far, no antibiotics have been developed that achieve this effectively. Previous experimental work has found a promising set of antibacterial peptides: $\beta^{2,2}$-amino acid derivatives, relatively small molecules with common structural elements composed of a polar head group and two non-polar hydrocarbon arms. In order to develop insight into possible mechanisms of action of these novel antibacterial agents, we have performed an *in silico* investigation of four leading $\beta^{2,2}$-amino acid derivatives, interacting with models of both bacterial (target) and eukaryotic (host) membranes, using molecular dynamics simulation with a model with all-atom resolution. We found an unexpected result that could shed light on the mechanism of action of these antimicrobial agents: the molecules assume a conformation where one of the hydrophobic arms is directed downward into the membrane core while the other is directed upwards, out of the membrane and exposed above the position of the membrane headgroups; we dubbed this conformation the "can-can pose". Intriguingly, the can-can pose was most closely linked to the choice of headgroup. Also, the compound previously found to be most effective against biofilms displayed the strongest extent of this behavior and, additionally, this behavior was more pronounced for this compound in the bacterial than in the eukaryotic membrane. We hypothesize that adopting the can-can pose could possibly disrupt the protective peptidoglycan macronet found on the exterior of the bacterial membrane.

1. Introduction

The emergence of strains of bacteria resistant to even the most powerful current antibacterial agents can be seen as one of the most serious crises facing humanity in the coming decades; the development of novel antibacterial drug therapies is an urgent priority. Additionally, microorganisms are now recognized to switch between two different lifestyles: a single-cell state, responsible for acute infections, and a multicellular state, associated with persistent diseases. The multicellular state is known as a *biofilm*, defined as an aggregated community of bacteria contained within a self-produced matrix [1]. Infections in the form of biofilms have been found to possess significantly higher tolerance to antibiotics and the host immune system [1]. As of yet, no antibiotic has been developed that effectively and selectively disrupt biofilms in human tissue. While the development of new antimicrobial agents is an urgent priority, the need for novel agents focused on the disruption of biofilms is even more pressing.

Antimicrobial peptides, or host defense peptides, are an ancient, in terms of evolution, component of the immune system of virtually all multicellular organisms [2]. They are thus considered as a promising source of new potent antibiotics: lead molecules in the design of peptidomimetics against highly resistant bacteria [3]. While the structural diversity of antimicrobials is significant, they are, in general, short, cationic and amphiphilic; *i.e.* they possess distinct hydrophilic and hydrophobic components: this allows them to bind to lipid-water interfaces [4]. The mechanism through which they perform their antimicrobial activity is multifaceted; it includes the disruption of the physical integrity of pathogen cell membranes, activation of host cell immune responses and induction of pleiotropic effects in a range of different cell types [4,5].

Several antibiotics based on antimicrobial peptides are currently in commercial development [6]. In spite of the fact that a considerable effort has been expended in their development over more than a decade, an unacceptable level of toxicity remains a problem; this limits the use of antimicrobial peptides in clinical settings, in particular, when administered orally [6,3]. A class of antibacterial peptides that has

* Corresponding author.
E-mail address: alex.bunker@helsinki.fi (A. Bunker).

https://doi.org/10.1016/j.bbamem.2019.07.016
Received 14 April 2019; Received in revised form 20 July 2019; Accepted 22 July 2019
Available online 31 July 2019

recently shown significant promise is $\beta^{2,2}$-amino acid derivatives [7,8,9]. These are relatively easy to produce, as they are small molecules with limited structural complexity. Thus, it can be expected that they would prove more suitable for oral administration, as suggested by phospholipid vesicle permeability assays [8,9]. Not only have they demonstrated high potency against planktonic Gram-positive and -negative bacterial cells, including methillin-resistant *S. aureus* bacteria, MRSA, but they have also, in particular, been found to be powerful biofilm disrupting agents [7]. Namely, the most potent $\beta^{2,2}$-amino acid derivative, labeled "A2 ", was demonstrated by Ausbacher et al., to be 16-fold more potent against *S. aureus* biofilms than penicillin G and resulted in an almost complete removal of bacterial cells at higher concentrations [7]. In that study, it was suggested that the small size of A2 would accelerate its diffusion into biofilms and that a membrane destabilizing effect could be responsible for its enhanced anti-biofilm activity; the exact mechanisms behind the anti-biofilm effect of A2, however, still remain unclear. Furthermore, the $\beta^{2,2}$-amino acid derivatives have low haemolytic activities against human red blood cells, thus showing the promise of reduced toxicity. While there is significant evidence of the potential of this class of antibacterial agents, their mode of action is, however, poorly understood; it has been suggested that $\beta^{2,2}$-amino acid derivatives, as in the case of some other antimicrobials, lyse bacterial cell membranes by disrupting their physical properties [7,4], however, other mechanisms cannot be excluded.

Obtaining a detailed mechanistic understanding of the activity of antimicrobial peptides, particularly their potential to disrupt biofilms, is extremely challenging; performing *in vitro* studies has proved to be a very daunting task for a number of reasons. For example, a given antimicrobial peptide may or may not display activity depending on the experimental conditions, which in turn can affect the ability of clinical isolates to form biofilms [10]. Computational molecular dynamics modelling (MD) provides a new, unique, window into supramolecular systems. It is able to provide insight into interactions, with atomistic resolution, that is not accessible experimentally; *in silico* methodologies can make progress where *in vitro* methodologies have, in the past, been limited. Modelling a section of a biomembrane is a mature tool in biophysics that can be used to study the behavior of different biomembranes and their interaction with drug, or other xenobiotic, molecules [11]. This technique has been used, in past work, to study the behavior and action of antimicrobials [12,13,14,15]. In order to obtain more insight into the mechanism of action of this class of antimicrobial agents, we have studied a set of $\beta^{2,2}$-amino acid derivatives interacting with mammalian- and bacterial-like lipid bilayers *in silico* through atomistic molecular dynamics simulation. Our goal is to reveal 1) their conformational features at the lipid-water interface and 2) specific interactions with phospholipids.

From the set of promising antimicrobial $\beta^{2,2}$-amino acid derivatives, we chose to model the compounds that have been previously coined as A2, A3, A5 and A6 [7]. The chemical structures of the four compounds are shown in Fig. 1; all compounds are amphiphilic in nature, with a hydrophilic C-terminal cationic head group and two hydrophobic hydrocarbon arms. Between the four compounds there are two separate head groups, one shared by compounds A2 and A3 (1,2-diaminoethane) and the other shared by A5 and A6 (*N,N*-dimethylaminoethanol) and two separate arm structures, one shared by A2 and A5 (2-naphthalene methylene side-chains) and the other shared by A3 and A6 (para-tert-butyl benzyl side-chains). The hydrophobic arms of A2 and A5 are more polar than those of A3 and A6 based on the octanol-water partitioning of A2 and A3 (3.4 vs. 3.7) [8]. In addition, the head group of compounds A5 and A6, with double methylation of the C-terminal end primary amine and introduction of an ester linkage, is less polar in comparison to that of A2 and A3, without methylation. Further, the presence of an ester linkage in compounds A5 and A6 renders the molecules less polar.

All of the four above mentioned antimicrobial compounds were found to be potent in destroying planktonic *S. aureus* cells and their biofilms, however, the selectivity of these compounds against bacteria, vs. their haemolytic activities, showed substantial differences. Compounds A2 and A5 were the most selective for the case of planktonic and biofilm bacterial cells, however, they were slightly less potent against planktonic bacterial cells, in comparison to compounds A3 and A6 [7]. Regarding anti-biofilm activities, the compounds A2 and A3 were more potent in destroying *S. aureus* biofilms than A5 and A6 [7]. Intriguingly, it had been shown by Hansen et al. that by increasing the hydrophobicity of the non-polar arms, more effective antimicrobials were acquired in the context of planktonic bacterial cells [8], a result confirmed by the study of Ausbacher et al. [7]. In contrast, concerning the polar component of the compounds, A5 and A6, with the less hydrophilic headgroup, were found by Ausbacher et al., [7] to have a ~ 25–33 % reduction in antimicrobial activity, in comparison to compounds A2 and A3. Thus, the experimental evidence clearly shows that potency against biofilms is more strongly correlated to the structure of the headgroup than to the nature of the hydrophobic tails. Regarding selectivity, i.e. potency against microbial target vs. potency against host cells, the reverse was found to be true: compounds A2 and A5 (2-naphthalene methylene side chains) had significantly enhanced selectivity against planktonic bacterial cells in comparison to that found for A3 and A6 (with para-tert-butyl benzyl side chains) [7].

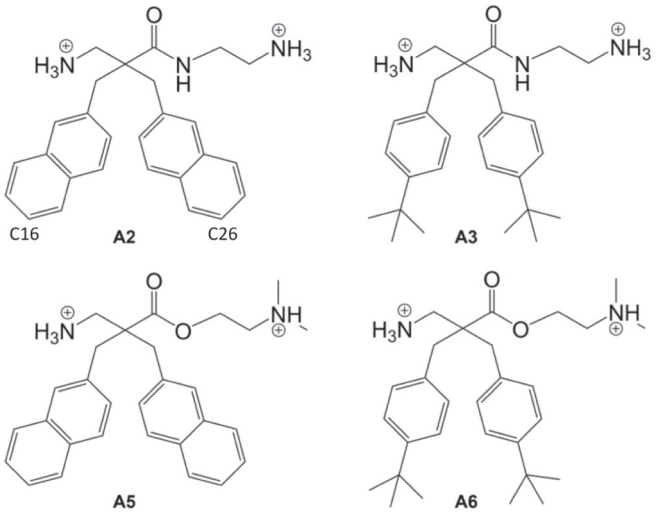

Fig. 1. The molecular structures for the four $\beta^{2,2}$-amino acid derivatives that we have studied in this contribution.

As $\beta^{2,2}$-amino acid derivatives are amphiphilic, it can be expected that they concentrate at the lipid-water interface of cell membranes and interact with the positively charged amine groups of the phospholipid (PL) head groups by plausibly forming salt bridges governed by ionic interactions and hydrogen bonds (H-bonds). Meanwhile, the hydrophobic tails are expected to interact with the acyl chains of PLs. A key to their mode of action is how the fashion in which they interact with both the membrane of the cells of the host and the membrane of the target bacteria differs; to shed light on this, we simulated the chosen antimicrobials interacting with mammalian- and bacterial-like lipid bilayers.

Though our simulations we found evidence that, while all compounds, as expected, located to the lipid-water interface, they exhibited unexpected differences in their behavior at the membrane surface. Specifically, they differed in the extent to which their hydrophobic arms were buried in the membrane core. In particular, the compounds were observed to sometimes display a conformation characterized by one arm directed down into the membrane while the other was thrust almost vertically out of the membrane, what we refer to as the "can-can pose" found, surprisingly, to be predominantly correlated to the choice of hydrophilic headgroup. Intriguingly, in addition to being more

prevalent in the compounds with the more hydrophilic headgroup (A2 and A3), for these compounds the prevalence of this conformation was also greater in the bacterial than the mammalian membranes, while the reverse was the case for compounds A5 and A6. These findings shed light on the mechanism behind the differences in the activity of these compounds and, hopefully, help pave the way for the development of yet even more effective antimicrobial agents.

2. Materials and methods

2.1. Systems simulated

We used computational molecular dynamics (MD) simulation to study the four compounds mentioned in the introduction interacting with two separate lipid membrane models, to study eukaryotic (mammalian, the patient or host) and prokaryotic (bacterial, the target) membranes respectively. In order to model the eukaryotic and prokaryotic lipid membranes we must approximate the lipid compositions in our simulations since incorporating thousands of different lipids species to MD simulations of lipid bilayers is, at least currently, out of reach at the moment. Thus, here we have chosen to use two-component lipid bilayer models to approximate mammalian and bacterial lipid membranes which, importantly, differ in surface charge. The eukaryotic model membrane was composed of 1 - palmitoyl - 2 - oleoyl - phosphathidylcholine (POPC) and cholesterol (CHOL) molecules; the prokaryotic model membrane was composed of 1 - palmitoyl - 2 - oleoyl - phosphathidylethanolamine (POPE) and 1 - palmitoyl - 2 - oleoyl - phosphathidylglycerol (POPG). Essentially, the total charge of eukaryotic model membrane is 0, whereas the total charge of the prokaryotic model membrane is negative.

Both POPC:CHOL and POPG:POPE molar concentration ratios were set to 3:1. All four antibacterial agents were simulated interacting with both the aforementioned mammalian and bacterial membrane models, for a total of eight systems; in each simulation ten of these molecules were added to the water phase of these systems. As the antibacterial agents and POPG have positive and negative charge respectively, for all systems either Cl^- or Na^+ ions were added to achieve charge neutrality.

To investigate the effect of initial conditions, additional simulations were performed, with four of the antibacterial agents positioned within the membrane core at the start of the simulation; while initialization with the compounds studied in the solvent is the best model of the real systems we study, the additional simulations with the molecules starting the simulation in the membrane core will provide additional insight. The compounds were inserted into the membrane core as follows: starting with a simulation with the compounds initialized in the water phase, we took a frame from the simulation after 1 μ s of simulation; four antimicrobials were pulled to the center of the bilayer so that both hydrophobic arms were buried in lipids in each case; all other antimicrobials were removed from the systems. A lower number of antimicrobials were used in the simulation where the molecules were initially placed into the lipid bilayer center, since placing 10+ highly charged molecules (the total charge of one antimicrobial is +2) into the center would disrupt the membrane structure; additionally, the resulting 20+ total charge in a hydrophobic phase without counter ions would result in a highly unphysical system.

Also, to insure that none of our observations were artefacts of the specific force field chosen, we repeated a subset of our simulations with two alternate force field parameter sets (details described below). We also simulated one system with physiological salt concentration present, to demonstrate that the presence of salt has no effect on the phenomena observed. In addition, we simulated two replica exchange simulations to show that the simulation with four A2 or A6 antimicrobials at the center of the bilayer initially converge to the same conformations as in the case of simulations where antimicrobials were initially placed in the water phase (see details and discussion in the Supplementary material). See Supplementary Table S1 in the Supplementary material (SM) for the full list of all systems simulated and number of each variety of molecule in each simulation.

2.2. Force field parameter sets

The complementary MacRog [16] and OPLS-AA [17] (optimized potentials for liquid simulations - All Atom) force fields were utilised for lipids and $\beta^{2,2}$-amino acid derivative molecules, respectively, in simulations carried out with all atom resolution; partial charges for $\beta^{2,2}$-amino acid derivates were parametrised using the Gaussian and Amber14 software packages [18,19]. First, the molecules were fully optimized at the Hartree-Fock (HF) level with the 6-31G* basis set. This was followed by calculation of atomic charges with the Merz-Kollman scheme [20] employing the HF level and 6-31G* basis set. The charges obtained in this way were replaced by the restrained electrostatic potential (RESP) charges. In this step, the Antechamber tool, included in the Amber14 modelling package, was used [19]. The Lennard-Jones and bonded parameters were based on the standard OPLS-parametrization [17]. We repeated a subset of our simulations using two alternative potential sets: the lipids modelled using Slipids [21,22] and Lipid14 [23] potentials, in each case with the antimicrobial agents modelled using the Generalized Amber Force Field (GAFF) [24], compatible with both these lipid potential sets; further details regarding the construction of these systems is found in SM, Section S1. For all potential sets considered, the same partial charges, calculated using the protocol described above, were used.

2.3. Simulation parameters

Molecular dynamics simulations were conducted using the GROMACS simulation package (version 5.1.2) [25,26]. All systems, including those carried out with the alternate potential sets, were first energy minimized using the steepest descent algorithm with 5000 minimisation steps. After this, short equilibration simulations were carried out to stabilise pressure fluctuations followed by 2 μ s of simulation at constant temperature and pressure. The time step was set to 2 fs; temperature and pressure were maintained at 310 K and 1 bar, respectively. Berendsen coupling schemes were utilised to achieve constant temperature and pressure during the short equilibration simulations [27]. After this, for the 2 μ s simulations, Nosé-Hoover and Parrinello-Rahman coupling algorithms were employed, to treat temperature and pressure, respectively [28,29]. Semi-isotropic pressure coupling was used. The coupling constants chosen, for the aforementioned thermostat and barostat, were 1 ps^{-1} and 12 ps^{-1}, respectively. Water, plus ions, lipids and antimicrobial compounds were coupled to separate heat baths. A cut-off of 1 nm was used for the Lennard-Jones interactions; electrostatic interactions were handled using the particle-mesh Ewald method with a real space cut-off of 1 nm [30]. The LINCS algorithm was applied to constrain bond lengths [31].

2.4. Analysis details

All the analysis programs listed here are part of the GROMACS simulation package [25,26]. The gmx_traj program was used for monitoring the center of mass of the antimicrobial agents as a function of time. In addition to this, the orientation of non-polar components of the antimicrobial agents were analyzed using the gmx_traj program. More specific calculation of the angles between the hydrophobic arms and the bilayer normal were calculated by using a code built in house (see Results 3 for further details). Mass density profiles were produced using the gmx_density program; the Z-axis of the simulation boxes were divided into 100 slices and the average number density, over the whole simulation trajectory, was calculated in each of them. The number of hydrogen bonds formed between selected atoms of the antimicrobial agents and lipids was determined using the gmx_hbond program; the

maximum distance between an H-bond donor and acceptor was set to 0.35 nm and the maximum angle formed by hydrogen bonding atoms (hydrogen-donor-acceptor) was set to 30 °, a standard, widely accepted, definition of an H-bond in the context of MD simulations carried out with all atom resolution [32,33,34]. Calculations of tilt angles of the polar head and non-polar arms of the antimicrobial agents, with respect to the lipid bilayer normal, were calculated using the gmx_gangle program. Radial distribution functions (RDFs) were determined using the gmx_rdf program. The lateral RDFs for all lipids around the antimicrobial compounds were determined; center of masses were used in all calculations. The gmx_sasa program was used to calculate the solvent accessible surface of the antimicrobial compounds. All visualization of molecular configurations was carried out using Visual Molecular Dynamics (VMD), version 1.9.3. [35]

3. Results

We first monitored a visualization of the trajectories for the eight systems studied; in every case the antimicrobial agents were seen to clearly locate to the position of the lipid headgroups. As shown in Supplementary Fig. S1 in SM, for both initial positions of the antimicrobials, solvent and membrane core, the position of the central carbon atom of all antimicrobials was seen to locate to the position of the phosphate headgroups of the lipids; in all cases this was seen to occur during the first μ -second of the simulation; for further details see SM, Section S2. Analysis of the raw time series data for all other calculated properties (more details below) also indicates that equilibration has roughly been achieved by the time 1 μ s has elapsed (again, see SM, Section S2); the results from the last microsecond of the 2 μ s simulation are thus used for all analysis. The results for the systems where the agents were initialized within the membrane did not, however, quantitatively match the results for the systems where the agents were initialized in the solvent (see SM, Section S3). We were, however, using the alternate potential set mentioned above, able to show convergence of the results from the two starting points; the Slipids + GAFF potential set, while obtaining the same static properties, sampled new conformations more quickly and we were able to accelerate the sampling further still using replica exchange in order to achieve this result, shown in the Supplementary materials, Fig. S12.

Our simulations conducted with physiological salt ion concentration (see SM, Section S4) show no effect on our results due to the presence of the ions. In the remainder of the simulations we carried out, we have not considered ions in the solution; investigation of any resulting effect would be problematic since the bacteria could be in several different ionic environments, *e.g.* in the intracellular environment the salt present is predominantly KCl while in the intercellular environment the salt present is predominantly NaCl. Our simulations carried out with the alternate potentials did not show any qualitatively different results concerning the static properties, however, the dynamics of these simulations was seen to occur more quickly (see SM, Section S4); since our analysis is not dependent on any dynamic observables, this is not an issue. The remainder of this paper thus discusses only the eight systems: each of the four agents studied, each interacting with both mammalian and bacterial membrane; the agents are initialized outside the membrane and the last μ-second of the simulated trajectories are considered for all analysis.

Now that it has been determined that the compounds all locate to the position of the membrane headgroups, we investigate further details regarding the orientation and behavior at the interface. As mentioned in the introduction, the compounds can all be divided into two components, a hydrophilic head and hydrophobic arms, as shown in Fig. 2A. We plotted the mass density profiles for both components of the compounds separately, relative to the position of the phosphate headgroup, as determined from the position of maximum density for the phosphate group for all eight systems, shown in Fig. 2B (see SM for full mass density profile results, Figs. S5 and S6). The mass density profile measures the relative densities of specific atoms, atom groups or molecules within the system along the membrane normal; it serves as a measure of where in the membrane these different elements sit. We see that, in all eight cases, the hydrophilic head sits just inside the membrane from the phosphate headgroup while the hydrophobic tails present a double peaked distribution, thus locating either outside or inside the membrane. Comparing the mass density profiles for the four different compounds, we see a striking difference that results from alteration of the hydrophilic head of the compound: the compounds A2 and A3, with the more polar head group, showed a significantly greater presence of the hydrophobic tail outside of the membrane than the case for compounds A5 and A6. Another useful quantity that can be calculated is the Solvent Accessible Surface Area (SASA), a measure of the relative surface area of atom group or molecule with the solvent. Results for the SASA for the components of each of the four compounds in both membranes, shown in Fig. 2C, corroborates the picture we see from the mass density profile results: compounds A2 and A3 show significantly greater exposure to the solvent by their hydrophobic arms. Interestingly, we see the reverse pattern concerning the exposure to the solvent of the hydrophilic head: SASA of the hydrophilic component is significantly greater for compounds A5 and A6 than for A2 and A3. Concerning the difference between behavior of the compounds in bacterial and mammalian membranes, we see, in all cases, both hydrophobic and hydrophilic components sit deeper in the membrane and have less exposure to the solvent, *i.e.* lower SASA, in the mammalian than in the bacterial membrane, thus all compounds penetrate more deeply into the mammalian than the bacterial membranes.

We next investigated the orientations of the two hydrophobic arms of the compounds, to determine the mechanisms through which they have their characteristic distribution, located either outside or inside the membrane. We defined two vectors, between the central carbon atom and the end carbon atoms of the two hydrophobic arms. For each of the eight systems, we constructed a heat map of angle between the membrane normal and each of the two vectors, with one on the x axis and the other on the y axis, shown in Fig. 3A. Analyzing this, we see two patterns of distribution: 1) one arm buried in the membrane, pointed down and the other pointed up out of the membrane and 2) both arms buried in the membrane. The compounds thus sometimes have both arms within the membrane and sometimes one out of the membrane, like a can-can dancer kicking her leg into the air (see images in Fig. 3A). We see that the extent to which the compounds are behaving in each of these fashions differs between the different systems, as shown in the differences between the heat maps; membranes where each of the two states are prevalent are visualized in Fig. 3B. In order to quantify this, we defined two states for the molecule: the molecule was in the “both arms buried” configuration when both end carbon atoms of the two hydrophobic arms were below the phosphate groups of lipids and “one arm buried” when one was above, what we dub as the “can-can pose ”. The results of the prevalence of the “both arms buried” configuration, in each system, is shown in Fig. 3C. We now see another striking difference between the compounds with the different hydrophilic headgroups (A2 and A3 vs. A5 and A6): for A2 and A3 the extent to which the “both arms buried” configuration is present is greater for the mammalian than bacterial membrane and for A5 and A6 this is reversed; once again, we see the dominant effect of the choice of hydrophilic headgroup.

Now that we have shown the important role the hydrophilic head group plays, we analyze the nature of the interaction between the hydrophilic headgroup and the membrane. As shown in Fig. 4A, the compounds A2 and A3 share a common hydrophilic headgroup with three H-bonding sites, while for A5 and A6 there are two H-bonding sites. In particular, the presence of two primary amines and one secondary amine in compounds A2 and A3 are able to form seven H-bonds, whereas A5 and A6 have one primary amine and one tertiary amine that are able to form four; in all cases the compounds possess H-bond donor sites (hydrogen atoms) that interact with the H-bond acceptor sites (oxygen atoms) in the membrane headgroups. In addition, we

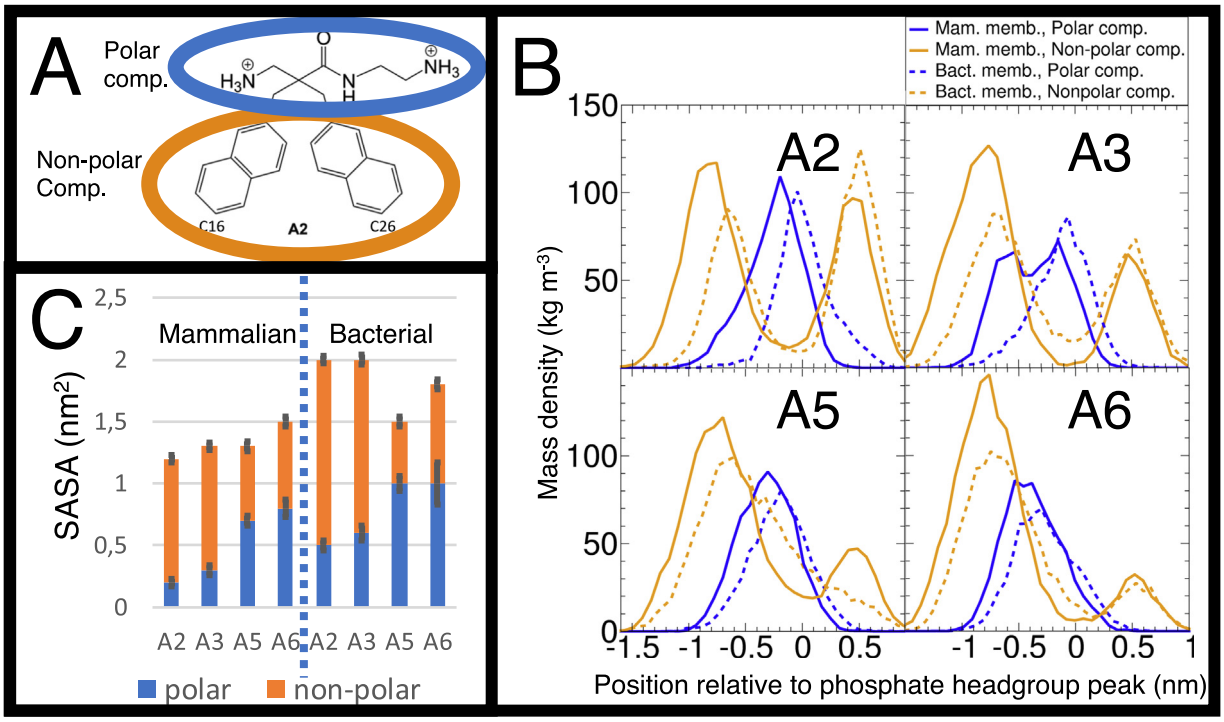

Fig. 2. Analysis of the positioning in the membrane of the hydrophilic and hydrophobic components of the four compounds, identified in part A, B) mass density profile results showing location within the membrane of the two components with respect to the position of the phosphate headgroup peak and C) the solvent accessible surface area (nm^2), i.e. area exposed to solvent outside the membrane, for the two components of each of the four compounds.

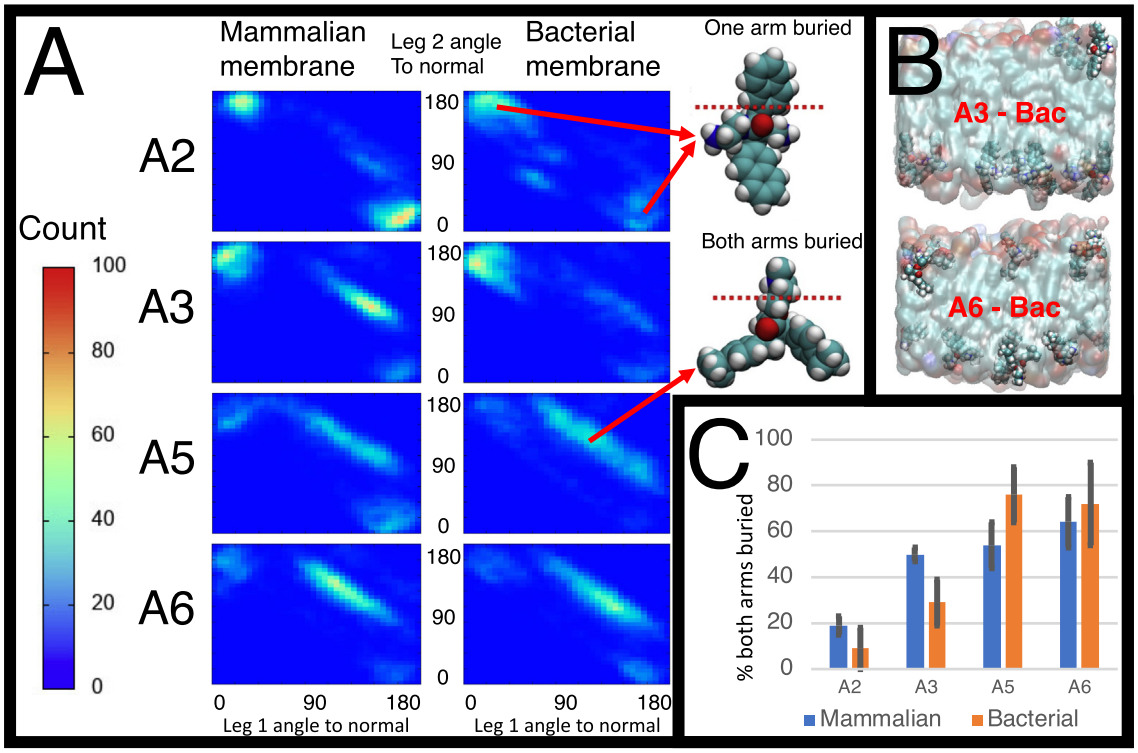

Fig. 3. Analysis of the relative orientation of the hydrophobic arms of the compounds: A) heat maps of the orientations of the two hydrophobic arms; the x and y axes are the angle of the first and second hydrophobic arms with the membrane normal respectively, B) visualization of the compounds A3 and A6 in the bacterial membrane, A3 shows a greater prevalence of the one arm buried, "can-can pose" configuration, C) bar graph of the percentage of instances of compounds in the two arms buried configuration for the four compounds in both mammalian and bacterial membranes.

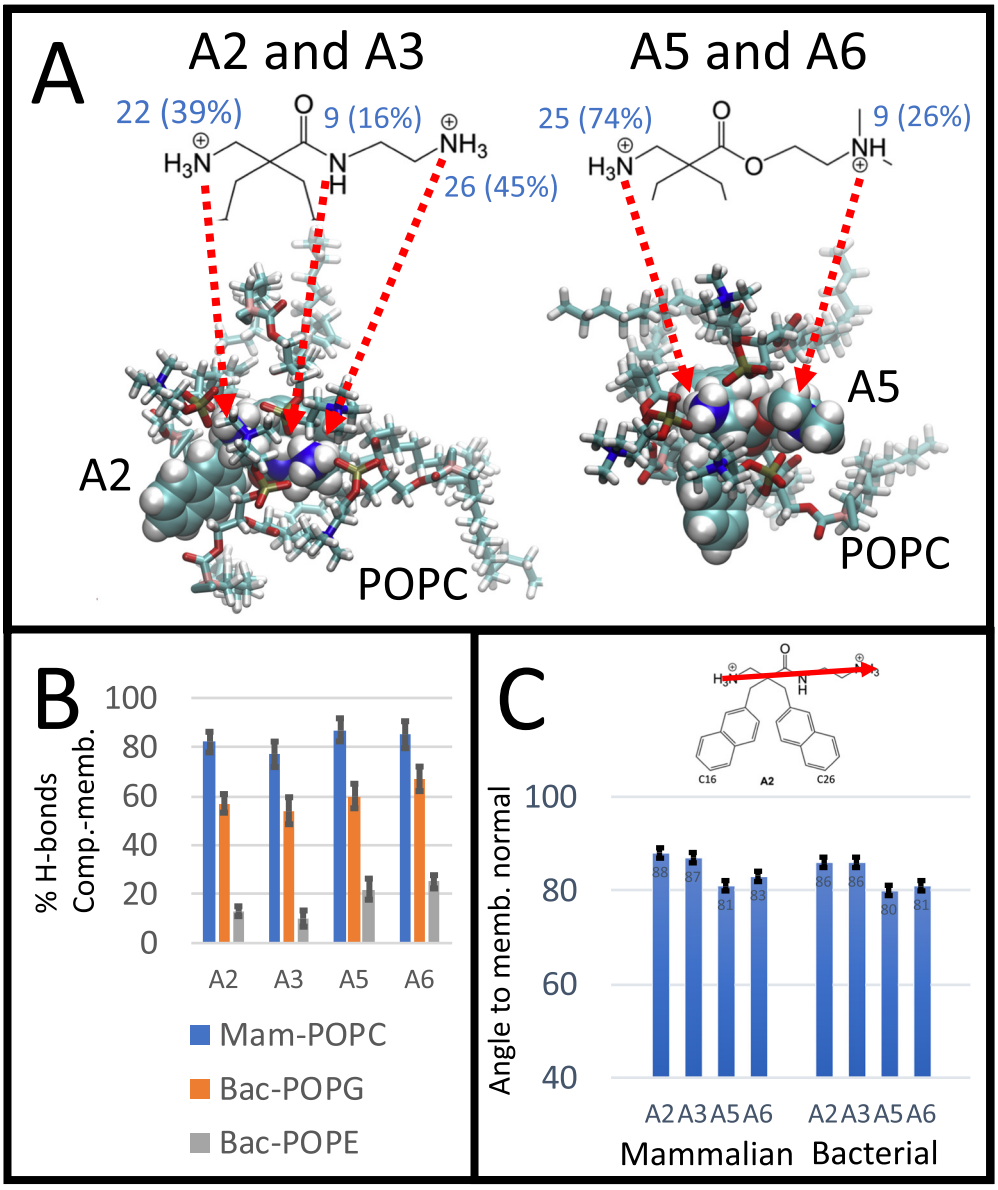

Fig. 4. Analysis of the interaction of the hydrophobic component of the compounds with the membrane headgroups: A) visualization of the H-bond forming sites for both headgroup types present, B) percentage of H-bonds between compounds and membrane headgroups, POPC for the mammalian headgroups and POPE and POPG for the bacterial membranes, C) orientation of the hydrophilic component of the compound.

must also consider the attractive electrostatic interaction between the positively charged amine groups of antimicrobials and the negatively charged phosphate groups of lipids. These, together with the formation of a number of hydrogen bonds, result in the formation of salt-bridges.

For the mammalian membrane, the compounds form H-bonds with the head groups of the POPC lipids and for the bacterial membranes, H-bonding occurs with both the POPG and POPE lipids. Corroborating the fact that the important dominant interactions are between the compound headgroups and the POPC or POPG/POPE lipids, results for the RDF between membrane molecules and the compounds show, as expected, that the compounds locate laterally in the membrane to the positions of these molecules and not to cholesterol (see SM, Section S5). We calculated the prevalence of these H-bonds, shown in Fig. 4B. Compounds A2 and A3 clearly form a higher number of H-bonds with POPC (77–82 % of total H-bonds), in the mammalian-like membrane environment, when compared to the total number of H-bonds formed with the bacterial-like membrane, comprised of POPG and POPE (64–70 % of total H-bonds). The difference, however, diminishes when studying H-bonds formed by compounds A5 and A6 in mammalian- and bacterial-like lipid environments (85–87 % vs. 82–92 %, respectively).

This result highlights the role of the more hydrophobic polar head group of A5 and A6 in their interaction with the lipid head groups. Namely, the less polar head groups of A5 and A6 form equally strong H-bonds with mammalian- and bacterial- membranes, whereas A2 and A3 form stronger H-bonds with mammalian membranes. In all systems, all H-bonding sites participate in binding the compound to the membrane as, in all cases, the H-bonding is primarily with the membrane lipid head groups (phosphate groups). As the interaction of antimicrobial amines with phosphate groups of lipids is also heavily governed with the attractive nature of the opposing total charges of the groups, the formation of salt-bridges is eminent. Thus, compounds are bound to the membrane through the formation of salt-bridges and H-bonding with the lipid head groups in addition to hydrophobic interactions between the arms of the compound and the hydrophobic core of the membrane.

The behavior of the hydrophilic head of the four compounds will play a key role in the overall behavior of the compounds. We have,

additionally, measured the angle of the hydrophilic head of the compounds in the membrane, shown in Fig. 4B; here, we see a striking difference between the two different headgroups: the A2 and A3 headgroup sits flatter in the membrane, closer to 90° from the membrane normal.

Altogether, we see the choice of hydrophilic headgroup to have more bearing on the interaction with the lipid membrane than the choice of hydrophobic arm. The headgroup of compounds A2 and A3 sits flatter in the membrane; it can be postulated that this altered orientation of the headgroup gives rise to the greater propensity for the compound to kick one of its arms out of the membrane: the can-can pose. Of particular importance is how this behavior differs in the bacterial and mammalian membrane; for compounds A2 and A3, with one headgroup type, the can-can pose is more prevalent in the bacterial membrane while for to other headgroup type, present in compounds A5 and A6, it is less prevalent in the bacterial membrane. We see less effect on the behavior of the compounds in the membrane resulting from the choice of hydrophobic arm, however, one notable effect is that compound A2 has a significantly greater occurrence of the can-can pose than compound A3.

4. Discussion and conclusion

We used MD simulation to study four $\beta^{2,2}$-amino acid derivatives that have previously been investigated experimentally [7,8,9] interacting with both models of bacterial and mammalian cell membranes; the goal was to obtain insight into how their interaction with the membranes of the target (bacterial, prokaryotic membrane) and the host (cell, eukaryotic membrane) may differ and how the behaviors of the compounds differ from each other. The structures of the compounds were differentiated by both the hydrophilic head group and hydrophobic tails. All compounds were seen to locate to the lipid-water interface, as was to be expected due to their amphiphilic nature. The compounds, however, exhibited a striking behavior that was not anticipated: in some cases one of the two hydrophobic arms was completely exposed to the water phase, directed outwards from the membrane, whereas the other arm was buried and directed towards the membrane core. We refer to this conformation as the “can-can pose ”. What predominantly differentiated these four compounds was the extent of the occurrence of this conformation and, more importantly, how this varied between the bacterial and cell membranes. Of particular note, we found that the dominant effect resulted from the structure of the hydrophilic headgroup rather than the hydrophobic arms: compounds A2 and A3, not only expressed a greater extent of the one-arm-buried conformation, but, more importantly, this conformation was more prevalent in the bacterial-like membrane than in the mammalian-like membrane while, for A5 and A6, this behavior, that exhibited itself to a much weaker extent, was reversed, *i.e.* more prevalent in the mammalian-like membrane than the bacterial-like membrane. Between compounds A2 and A3, compound A2 exhibited this phenomenon to a stronger extent than A3; this was to be expected as A2 possesses the slightly less hydrophobic 2-naphthalene methylene arms, as indicated by the octanol-water partition coefficients [8].

These findings provide new mechanistic insight that can possibly explain the efficacy of A2 and A3 as selective antimicrobial agents. An essential factor regarding their efficacy is the ability of these compounds to preferentially interact with the target bacterial membranes in a disruptive manner and to display a, relatively, reduced affinity towards the mammalian cell membranes of the host organisms. As described in the introduction, the previously described experimental studies [7] found that compounds A2 and A3 showed significantly superior biocidal efficacy against bacterial biofilms, in comparison to compounds A5 and A6; efficacy is thus predominantly correlated with the choice of polar headgroup. On the other hand, selectivity was found to be superior for compounds A2 and A5; selectivity is thus predominantly correlated to the choice of hydrophobic arms [7]. In our simulation studies the prevalence of the can-can pose was predominantly correlated to the choice of polar headgroup, thus this phenomenon may be more closely related to efficacy than selectivity.

At this point, it is necessary to clarify what precisely, in this case, MD simulation is and is not, capable of. What we have is a model, given a set of assumptions, that isolates a specific element of the system being studied. This is not a realistic visualization of all aspects of what happens when these antimicrobial agents encounter bacterial and cell membranes, but rather a model for the behavior of individual compound molecules, in isolation, at simplified model formulations of bacterial and cell membranes. We have identified that a specific behavior, the can-can pose, correlates to efficacy of the compounds towards bacterial biofilms; while this behavior, in isolation, is not the sole mechanism of antimicrobial activity, it may play an important role in the overall mechanism of activity. It is possible that differences in the extent of the overall polarity of the specific antimicrobial molecule could play a role in their selectivity and potency, however, we would argue that it is highly unlikely that this is the sole explaining factor as, in all simulations, all antimicrobials rapidly located to the lipid-water interface; this indicated that all compounds possessed strong lipid bilayer affinities for both membrane types. This issue is to be quantitatively investigated through a combination of experimental and computational methodologies in future work. Additionally, it is possible that, while the model membranes we constructed are designed to highlight the different properties of mammalian and bacterial membranes, aspects of the membranes not included in the study could alter our results; in some cases it has been found that such simplified membrane models have failed to correctly model key aspects of the properties of the membrane [36].

The primary effect of the adoption of the can-can pose is the exposure of a hydrophobic arm outside the membrane. Two possible outcomes that lead to bactericidal effects can be hypothesized: either this could 1) induce local aggregation of the compounds driven by the hydrophobic effect, resulting in a large scale collective behavior that disrupts the bacterial membrane structure or 2) the exposed hydrophobic arm outside the bacterial membrane could itself have a bactericidal effect. The latter hypothesis is particularly intriguing as it fits in well with our current understanding of the mode of action of antibacterial agents. Bacteria express a protective peptidoglycan layer outside of their cell membrane that forms a quasi-two-dimensional crystal structure known as a macronet. The mode of action of conventional antibiotics, including β-lactams (e.g., penicillins and cephalosporins), glycopeptides (e.g., vancomycin and teicoplanin) and daptomycin, is to inhibit the activity of key enzymes that play a role in the construction of the macronet. Antimicrobial peptides are not peptidoglycan synthesis inhibitors; they display a different mode of action. It has been suggested that they instead directly disrupt the structure of the peptidoglycan macronet in single-cells [37], direct experimental evidence, however, remains lacking. It is thus possible that the $\beta^{2,2}$-amino acid derivatives we have studied could be directly disrupting the macronet through contact with the hydrophobic arm of the agent that is exposed outside the membrane when it adopts the can-can pose.

Beyond the immediate mechanism we have found here, relating to these specific compounds, this can be seen as a case study of how *in silico* modelling using the MD simulation method with all atom resolution, can play a role in the development of novel anti-bacterial agents. Previously, a number of antimicrobial peptides have been simulated with lipid bilayers, indicating that most of the antimicrobial peptides bind to the lipid-water interface with the help of electrostatic and hydrophobic interactions; the cationic residues interact with negatively charged phosphate groups of phospholipids, whereas hydrophobic residues become buried within the lipid core of the membrane [12,13,14,15]. In addition, the importance of hydrogen bonding between cationic residues of the antimicrobial peptides and the phosphate oxygens of lipids, has been shown for the case of magain2 and MSI-78 [38]. Furthermore, the formation of Lys-phosphate salt bridges was

reported when transportan10 localized to the lipid-water interface[15]. In general, our results here agree with the previously performed studies. In this study, however, we report a novel behavior for a set of short $\beta^{2,2}$-amino acid derivatives at the lipid-water interface that contradicts the general amphiphilic view of antimicrobial peptides. Namely, the complete burial of all hydrophobic tails is not necessary for efficient antimicrobial activity. As mentioned above, the hydrophobic residues that protrude from the membrane could even play an important role in the yet unknown mode of action of $\beta^{2,2}$-amino acid derivatives. This novel feature might prove to be useful for designing more efficient antimicrobials in the future.

Transparency document

The Transparency document associated with this article can be found, in online version.

Acknowledgments

Academy of Finland, grants, 298863 (AK), 287963 (AB) and the Jane and Aatos Erkko Foundation (AF) have provided financial support. All computational resources provided by the Finnish IT Centre for Science Ltd. (CSC). We thank Aniket Magarkar for helpful advice.

Supplementary data

Supplementary data to this article can be found online at https://doi.org/10.1016/j.bbamem.2019.07.016.

References

[1] M. Alhede, K.N. Kragh, K. Qvortrup, M. Allesen-Holm, M. van Gennip, L.D. Christensen, P.O. Jensen, A.K. Nielsen, M. Parsek, D. Wozniak, S. Molin, T. Tolker-Nielsen, N. Høiby, M. Givskov, T. Bjarnshol, Phenotypes of non-attached Pseudomonas aeruginosa aggregates resemble surface attached biofilm, PLoS ONE 6 (11) (2011) e27943.
[2] A. Nijnik, R.E.W. Hancock, Host defence peptides: antimicrobial and immunomodulatory activity and potential applications for tackling antibiotic-resistant infections, Emerg. Health Threat. J. 2 (1) (2009) 7078.
[3] R.E.W. Hancock, H.-G. Sahl, Antimicrobial and host-defense peptides as new anti-infective therapeutic strategies, Nat. Biotechnol. 24 (2006) 1551.
[4] M. Zasloff, Antimicrobial peptides of multicellular organisms, Nature 415 (2002) 389.
[5] R.E.W. Hancock, E.F. Haney, E.E. Gill, Nat. Rev. Immunol. 16 (2016) 321.
[6] M. Zasloff, Antimicrobial Peptides: Do They Have a Future as Therapeutics? Springer International Publishing, 2016.
[7] D. Ausbacher, A. Fallarero, J. Kujala, A. Määttänen, J. Peltonen, M.B. Strøm, P.M. Vuorela, Staphylococcus aureus biofilm susceptibility to small and potent $\beta^{2,2}$-amino acid derivatives, Biofouling 30 (1) (2014) 81–93.
[8] T. Hansen, D. Ausbacher, G.E. Flaten, M. Havelkova, M.B. Strøm, Synthesis of cationic antimicrobial $\beta^{2,2}$-amino acid derivatives with potential for oral administration, J. Med. Chem. 54 (3) (2011) 858–868.
[9] L. Hanski, D. Ausbacher, T.M. Tiirola, M.B. Strøm, P.M. Vuorela, Amphipathic $\beta^{2,2}$-amino acid derivatives suppress infectivity and disrupt the intracellular replication cycle of Chlamydia pneumoniae, PLoS One 11 (6) (2016) 1–15.
[10] G. Batoni, G. Maisetta, S. Esin, Antimicrobial peptides and their interaction with biofilms of medically relevant bacteria, Biochim. Biophys. Acta Biomembr. 1858 (2016) 1044–1060.
[11] G. Enkavi, M. Javanen, W. Kulig, T. Róg, I. Vattulainen, Multiscale simulations of biological membranes: the challenge to understand biological phenomena in a living substance, Chem. Rev. (2019) ASAP.
[12] E. Matyus, C. Kandt, D.P. Tieleman, Computer simulation of antimicrobial peptides, Curr. Med. Chem. 14 (26) (2007) 2789–2798.
[13] B. Orioni, G. Bocchinfuso, J.Y. Kim, A. Palleschi, G. Grande, S. Bobone, Y. Park, J.I. Kim, K.-S. Hahm, L. Stella, Membrane perturbation by the antimicrobial peptide pmap-23: a fluorescence and molecular dynamics study, Biochim. Biophys. Acta Biomembr. 1788 (7) (2009) 1523–1533.
[14] G. Bocchinfuso, A. Palleschi, B. Orioni, G. Grande, F. Formaggio, C. Toniolo, Y. Park, K.-S. Hahm, L. Stella, Different mechanisms of action of antimicrobial peptides: insights from fluorescence spectroscopy experiments and molecular dynamics simulations, J. Pept. Sci. 15 (9) (2009) 550–558.
[15] C.M. Dunkin, A. Pokorny, P.F. Almeida, H.-S. Lee, Molecular dynamics studies of transportan 10 (tp10) interacting with a popc lipid bilayer, J. Phys. Chem. B 115 (5) (2011) 1188–1198.
[16] A. Maciejewski, M. Pasenkiewicz-Gierula, O. Cramariuc, I. Vattulainen, T. Rog, Refined opls all-atom force field for saturated phosphatidylcholine bilayers at full hydration, J. Phys. Chem. B 118 (17) (2014) 4571–4581.
[17] W.L. Jorgensen, D.S. Maxwell, J. Tirado-Rives, Development and testing of the opls all-atom force field on conformational energetics and properties of organic liquids, J. Am. Chem. Soc. 118 (45) (1996) 11225–11236.
[18] M. Frisch, G. Trucks, H. Schlegel, G. Scuseria, M. Robb, J. Cheesemman, et al., Gaussian 09, Revision E.01, Gaussian, Inc., Wallingford CT, 2013.
[19] J. Wang, W. Wang, P.A. Kollman, D.A. Case, Automatic atom type and bond type perception in molecular mechanical calculations, J. Mol. Graph. Model. 25 (2) (2006) 247–260.
[20] U.C. Singh, P.A. Kollman, An approach to computing electrostatic charges for molecules, J. Comput. Chem. 5 (2) (1984) 129–145.
[21] J.P.M. Jämbeck, A.P. Lyubartsev, Derivation and systematic validation of a refined all-atom force field for phosphatidylcholine lipids, J. Phys. Chem. B 116 (10) (2012) 3164–3179.
[22] J.P.M. Jämbeck, A.P. Lyubartsev, An extension and further validation of an all-atomistic force field for biological membranes, J. Chem. Theory Comput. 8 (8) (2012) 2938–2948.
[23] C.J. Dickson, B.D. Madej, Å.A. Skjevik, R.M. Betz, K. Teigen, I.R. Gould, R.C. Walker, Lipid14: the amber lipid force field, J. Chem. Theory Comput. 10 (2) (2014) 865–879.
[24] W. Junmei, R.M. Wolf, J.W. Caldwell, P.A. Kollman, D.A. Case, Development and testing of a general amber force field, J. Comput. Chem. 25 (9) (2004) 1157–1174.
[25] H.J. Berendsen, D. van der Spoel, R. van Drunen, GROMACS: a message-passing parallel molecular dynamics implementation, Comput. Phys. Commun. 91 (1-3) (1995) 43–56.
[26] B. Hess, C. Kutzner, D. Van Der Spoel, E. Lindahl, GROMACS 4: algorithms for highly efficient, load-balanced, and scalable molecular simulation, J. Chem. Theory Comput. 4 (3) (2008) 435–447.
[27] H.J.C. Berendsen, J.P.M. Postma, W.F. van Gunsteren, A. DiNola, J.R. Haak, Molecular dynamics with coupling to an external bath, J. Chem. Phys. 81 (8) (1984) 3684–3690.
[28] D.J. Evans, B.L. Holian, The Nose-Hoover thermostat, J. Chem. Phys. 83 (8) (1985) 4069–4074.
[29] M. Parrinello, A. Rahman, Polymorphic transitions in single crystals: a new molecular dynamics method, J. Appl. Phys. 52 (12) (1981) 7182–7190.
[30] U. Essmann, L. Perera, M.L. Berkowitz, T. Darden, H. Lee, L.G. Pedersen, A smooth particle mesh Ewald method, J. Chem. Phys. 103 (19) (1995) 8577–8593.
[31] B. Hess, H. Bekker, H.J.C. Berendsen, J.G.E.M. Fraaije, LINCS: a linear constraint solver for molecular simulations, J. Comput. Chem. 18 (12) (1997) 1463–1472.
[32] K. Murzyn, T. Róg, G. Jezierski, Y. Takaoka, M. Pasenkiewicz-Gierula, Effects of phospholipid unsaturation on the membrane/water interface: a molecular simulation study, Biophys. J. 81 (1) (2001) 170–183.
[33] K. Modig, B.G. Pfrommer, B. Halle, Temperature-dependent hydrogenbond geometry in liquid water, Phys. Rev. Lett. 90 (7) (2003) 075502.
[34] D. van der Spoel, P.J. van Maarten, N. Tîmneanu, Thermodynamics of hydrogen bonding in hydrophilic and hydrophobic media, J. Phys. Chem. B 110 (9) (2006) 4393–4398.
[35] W. Humphrey, A. Dalke, K. Schulten, Vmd: visual molecular dynamics. J. Mol. Graph. 14 (1) (1996) 33–38.
[36] A.N. Leonard, E. Wang, V. Monje-Galvan, J.B. Klauda, Developing and testing of lipid force fields with applications to modeling cellular membranes, Chem. Rev. 119 (2019) 6227–6269.
[37] N. Malanovic, K. Lohner, Gram-positive bacterial cell envelopes: the impact on the activity of antimicrobial peptides, Biochim. Biophys. Acta Biomembr. 1858 (2016) 936–946.
[38] S.K. Kandasamy, R.G. Larson, Binding and insertion of alphahelical antimicrobial peptides in popc bilayers studied by molecular dynamics simulations, Chem. Phys. Lipids 132 (1) (2004) 113–132.